Review Article

ADVANCED PHOTONICS

Integrated continuous-variable quantum light sources for quantum computing

Xuezhi Zhu,[a] Siyu Ren,[a] Yunyun Cao,[a] and Xiaolong Su[a,b,*]
[a]Shanxi University, Institute of Opto-Electronics, State Key Laboratory of Quantum Optics Technologies and Devices, Taiyuan, China
[b]Shanxi University, Collaborative Innovation Center of Extreme Optics, Taiyuan, China

Abstract. Continuous-variable (CV) quantum light sources are the essential resource for quantum computation. Integrated CV quantum light sources offer a scalable pathway by harnessing low-loss nonlinear materials, versatile device architectures, and CMOS-compatible fabrication processes enabled by integrated photonics platforms. In this review, we briefly introduce recent progress on integrated CV quantum light sources, including single-mode squeezed states, two-mode squeezed states, and multimode entangled states. The key performance metrics of CV quantum light sources, such as the squeezing level, bandwidth, purity, and mode multiplexing, are analyzed. We highlight representative implementations of lithium niobate, silicon nitride, and silica platforms for CV quantum light sources and discuss major challenges for realizing integrated large-scale and fault-tolerant CV quantum computation.

Keywords: quantum information; quantum computation; integrated photonics; squeezed state; entangled state; cluster state.

Received Aug. 26, 2025; revised manuscript received Oct. 1, 2025; accepted for publication Oct. 20, 2025; published online Nov. 13, 2025.

[DOI: 10.1117/1.AP.7.6.064005]

1 Introduction

Optical quantum information processing can be categorized into discrete-variable (DV) and continuous-variable (CV) approaches, depending on whether the eigenvalues of the physical observables carrying quantum information are discrete or continuous. There are complementary advantages and disadvantages of quantum information processing based on the DV and CV systems,[1–4] which are developing in parallel. DV photonic systems encode information in a finite-dimensional Hilbert space to form the qubit, which naturally enables high-fidelity qubit operations, but the probabilistic generation of entangled states constrains the scalability. By contrast, CV photonic systems encode information in an infinite-dimensional Hilbert space, typically in the quadratures of optical fields to form the quantum mode (qumode). Although the fidelity of CV photonic quantum information processing with entangled states is limited, the deterministic preparation of entangled states enables scalable quantum computation[5–8] and quantum simulation.[9–12]

As an important architecture for quantum computation, measurement-based quantum computation (MBQC) implements computing on a large-scale entangled state known as a cluster state.[13,14] In the CV regime, large-scale cluster states can be deterministically generated from optical modes. For example, one-dimensional CV cluster state with 16,000 qumodes,[15] two-dimensional CV cluster state with up to 30,000 qumodes,[16,17] and even three-dimensional CV cluster state have been successfully demonstrated.[18] In addition, CV optical entangled states can be efficiently detected and characterized using room-temperature, high-efficiency homodyne detectors. These advantages have fueled growing interest in CV-based protocols across quantum communication,[19] sensing,[20] and computing.[21,22]

Toward practical optical quantum computation, the integrated photonic chip is increasingly recognized as an essential step for realizing compact and stable CV quantum hardware.[23,24] As shown in Fig. 1, integrated quantum photonic circuits offer inherent phase stability, high component density, and compatibility with complementary metal-oxide-semiconductor (CMOS) fabrication processes. These platforms enable the monolithic co-integration of nonlinear sources, phase shifters, and detectors, which reduces optical losses and phase drift while supporting scalability for integrated CV quantum photonics.

Among integrated CV quantum photonic material platforms, lithium niobate ($LiNbO_3$) stands out for second-order $\chi^{(2)}$

*Address all correspondence to Xiaolong Su, suxl@sxu.edu.cn

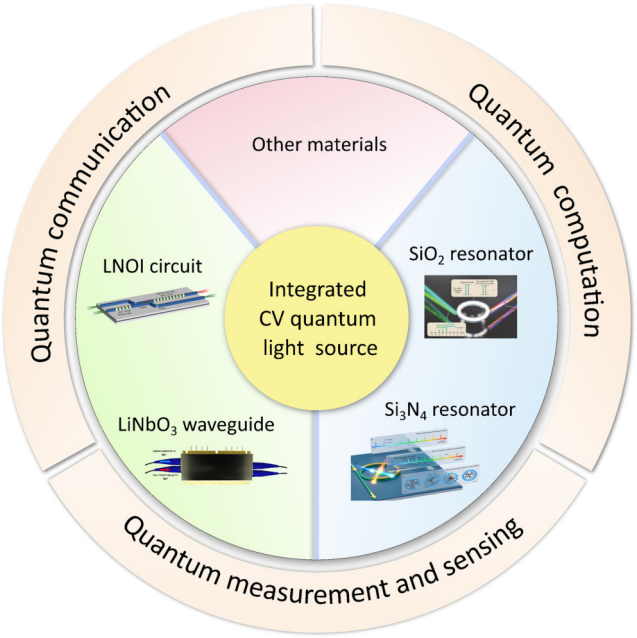

Fig. 1 Mainstream material platforms for CV quantum light sources. Panels reproduced with permission from Refs. 25–28.

nonlinear processes. Whether integrated-packaged $LiNbO_3$ or thin-film $LiNbO_3$ on insulator (LNOI), its high nonlinear coefficient and strong electro-optic effect facilitate squeezed light generation alongside on-chip modulation and amplification,[25,29–31] enabling high-quality quantum light sources, electrically tunable phase control, and robustness against losses. In particular, LNOI, through thin-film lithium niobate on insulator, provides rich functionalities in an integrated manner.[32] For third-order $\chi^{(3)}$ nonlinear processes, silicon photonic platforms, particularly silicon nitride (Si_3N_4) and silicon dioxide (SiO_2), are good candidates. The on-chip generation of reconfigurable CV cluster states and Gottesman–Kitaev–Preskill (GKP) states has been demonstrated recently.[26,33] These materials provide ultra-low propagation loss, mature fabrication workflows, and support for complex on-chip quantum circuits, from state generation to integrated detection.[34–36] Taken together, these advances highlight the potential of integrated photonics for scalable quantum computing.[24,37]

In this review, we focus on recent representative advances in CV quantum light sources based on $LiNbO_3$, Si_3N_4, and SiO_2 material platforms, the techniques, and the critical challenges to enable CV quantum computation. The paper is organized in the following structure. An overview of integrated single-mode squeezed light sources is provided in Sec. 2. Two-mode squeezed (CV entangled) light sources are discussed in Sec. 3. Integrated multipartite entangled light sources are covered in Sec. 4. Discussion and outlook are presented in Sec. 5.

2 Integrated Single-Mode Squeezed Light Sources

Single-mode squeezed states constitute the foundational resource for CV quantum information processing. The squeezing level of a squeezed state quantifies the reduction in quantum fluctuations (noise) of one quadrature relative to the vacuum noise. According to the Heisenberg uncertainty principle, this reduction is accompanied by an increase in fluctuations in the canonically conjugate quadrature, characterized by the anti-squeezing level.[38] For an ideal pure squeezed state, the squeezing and anti-squeezing levels are symmetric on a logarithmic scale. However, imperfections and decoherence in practical systems unavoidably decrease state purity, resulting in mixed states. In such cases, the purity becomes a crucial metric for evaluating the quality of the quantum state. Achieving squeezed states with both high squeezing and purity is essential for suppressing quantum noise and ensuring high-fidelity operations, which are critical prerequisites for reaching the fault tolerance threshold necessary for scalable quantum computation.[21,22]

Devices on various materials, such as mechanically polished periodically poled $LiNbO_3$ (PPLN) waveguide, LNOI waveguide, and Si_3N_4 resonator, have been developed to generate single-mode squeezed states, as shown in Fig. 2. Currently, mechanically polished and packaged $LiNbO_3$ waveguides, as shown in Fig. 2(a), can generate squeezed states with squeezing levels up to 8.3 dB.[41] Benefiting from the large $\chi^{(2)}$ nonlinear coefficient and broad quasi-phase-matching bandwidth of the parametric down-conversion process, squeezed states with several terahertz squeezing bandwidths have been demonstrated.[27] Such fiber-coupled squeezed light source modules and broadband squeezing enable higher data rates, thereby supporting faster quantum communication and computation.[42]

LNOI offers better device density and compatibility with scalable photonic integration and standardized fabrication. The reduced optical mode volume in LNOI structures enhances nonlinear interaction efficiency, and the platform allows for more flexible dispersion engineering, including higher-order flattening.[43] The integration of filters, phase shifters, and programmable beam splitters around on-chip squeezing sources has also been demonstrated, as illustrated in Figs. 2(b) and 2(c).[31,39] In addition, broadband detection using phase-sensitive amplification, as shown in Fig. 2(d), enables the conversion of squeezed states into macroscopic signals resilient to loss, resulting in the observation of over 25 THz squeezing bandwidth, with a maximum squeezing level of 4.9 dB.[25] With ongoing improvements in surface quality, fabrication precision, and material uniformity, fully integrated LNOI CV quantum photonic platforms are becoming increasingly feasible.

Beyond $LiNbO_3$, silicon-based photonic platforms offer an alternative approach to generate squeezed light, benefiting from mature CMOS-compatible fabrication and different nonlinear mechanisms.[44] Due to their centrosymmetric crystal lattice structures, single-mode squeezed states can be generated via four-wave mixing (FWM) processes driven by bichromatic pumping, which excites frequency-degenerate quantum modes, as shown in Fig. 2(e).[34] Owing to the intrinsically weak $\chi^{(3)}$ nonlinearity, these platforms typically employ resonant structures to enhance the nonlinear interaction, such as microring resonators,[45] whispering-gallery-mode resonators,[46] Fabry–Pérot cavities,[47] and photonic crystal cavities.[48] Leveraging scalable commercial fabrication, these systems can integrate squeezed light sources with auxiliary elements such as Mach–Zehnder interferometers or additional microresonators to meet various requirements for programmable squeezing level, state purity, and coupling tunability.

Among silicon-compatible materials, Si_3N_4 stands out for its superior optical properties, including low nonlinear loss, broad transparency window, and the absence of two-photon absorption, making it a compelling candidate for squeezed light

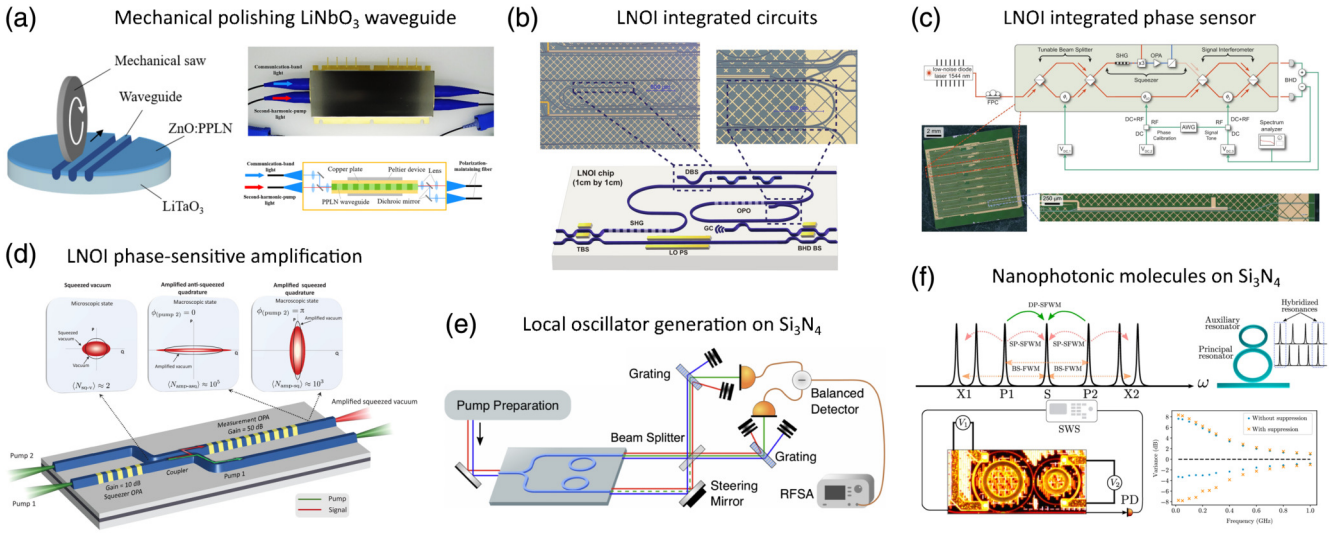

Fig. 2 Typical integrated single-mode squeezed state sources. (a) Low-loss quasi-single-mode periodically poled $LiNbO_3$ (PPLN) waveguide within a fiber packaged optical parametric amplification module.[27] (b) Degenerate squeezed light generation and tomography by implementing an integrated photonic circuit incorporating an optical parametric oscillator.[39] (c) LNOI photonic integrated circuit, containing a PPLN optical parametric amplification waveguide, performing a quantum-enhanced measurement, and achieving signal-to-noise-ratio improvement.[31] (d) An integrated nanophotonic platform based on LNOI to generate and all-optically measure squeezed states on the same optical chip.[25] (e) Generation of quadrature-phase squeezed states in the radio-frequency carrier sideband using a small-footprint Si_3N_4 microresonator with a dual-pumped FWM process.[34] (f) A photonic molecule composed of two coupled microring resonators, designed to generate strongly squeezed light uncontaminated by noise from unwanted parasitic nonlinear processes.[40]

sources. Nanophotonic molecules fabricated on Si_3N_4 exploit avoided mode crossings to dynamically tune coupling conditions and mode splittings, enabling programmable control of squeezing.[49] By suppressing parasitic nonlinear effects beyond degenerate FWM,[40] 1.65 dB (8 dB inferred on-chip) of squeezing was achieved only at approximately half the optical parametric oscillation threshold, as shown in Fig. 2(f). These features in programmability and scalability present particular advantages for the realization of multiplexed CV cluster states.

3 Integrated Two-Mode Squeezed Light Sources

The two-mode squeezed state (TMSS) is the smallest-scale entangled state in the CV regime. For the TMSSs, the joint fluctuations of certain linear combinations of the quadratures are reduced below the corresponding standard quantum limit, whereas individual modes of the TMSS are thermal states. It has been shown that TMSS has broad applications in quantum key distribution, quantum teleportation, and quantum nondemolition gate.[50,51] In addition to generating TMSSs by applying a beam splitter to two single-mode squeezed states, as shown in Fig. 3(a),[52] integrated CV quantum photonic systems also typically produce phase-stable frequency-mode pairs within a single spatial mode through nondegenerate parametric down-conversion or FWM, as shown in Figs. 3(b) and 3(c).[45,53]

Benefiting from the small mode volume and engineered structural dispersion, integrated devices such as waveguides, resonators, and couplers can operate over a much broader frequency range compared with bulk optics, thereby enabling the simultaneous generation of multiple TMSSs. For example, a 3 mm diameter SiO_2 wedge resonator with a 22 GHz free spectral range (FSR) has been demonstrated, as shown in Fig. 3(d). Within a 1 THz optical span at telecommunication wavelengths, this device generates 40 CV quantum frequency modes in the form of 20 simultaneously two-mode squeezed comb pairs.[46] By employing a tapered fiber, the coupling condition can be dynamically adjusted, resulting in a maximum observed squeezing level of 1.6 dB.

In addition to spectral multiplexing, the control of temporal modes is also important for applications requiring high mode purity. Owing to the broader phase-matching bandwidth of the nonlinear process compared with the bandwidth of the excitation field, the resulting quantum modes exhibit frequency anti-correlation and enable a high photon pair generation rate. The strong pumping required for TMSS generation induces self- and cross-phase modulation, which can be exploited to engineer the temporal mode of the output quantum state. By appropriately adjusting the pulse width of the pump, as shown in Fig. 3(e), it is possible to approach single temporal mode output, thereby satisfying the mode purity requirements of various quantum sampling tasks, such as Gaussian Boson sampling.[55]

Even under ideal conditions, fault-tolerant CV quantum computation requires a squeezing level of at least 10 dB.[57] This limitation is largely attributed to excess noise introduced by thermal fluctuations, pump phase instability, and self-phase modulation under strong pumping conditions.[58] To mitigate these effects, strategies such as reducing resonator size and stabilizing pump

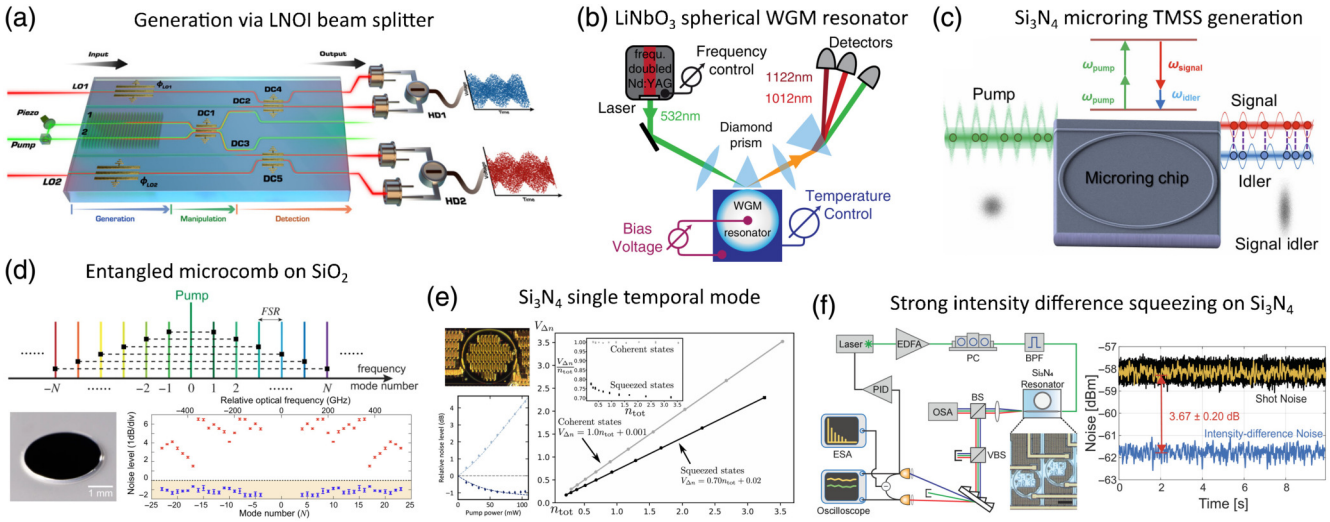

Fig. 3 Typical integrated two-mode squeezed state sources. (a) A dynamically reconfigurable waveguide network generates a two-mode entangled state.[52] (b) A spherical whispering gallery mode (WGM) resonator pumped far above threshold generates intensity squeezing of each parametric beam and squeezing of twin-beam quantum correlations.[53,54] (c) A microring FWM optical parametric oscillator pumped above threshold generates sub-shot-noise quantum correlations between bright twin beams.[45] (d) A deterministic quantum microcomb in a SiO_2 microresonator on a silicon chip, consisting of 20 TMSS comb pairs, within 1 THz optical span at telecommunication wavelengths.[46] (e) A Si_3N_4 microring resonator driven spontaneous FWM below threshold generates TMSS and photon number difference squeezing.[55] (f) A foundry-fabricated Si_3N_4 microring with 3.7 dB (10.2 dB inferred on-chip) intensity difference squeezed state.[56]

detuning have been employed. A representative example is shown in Fig. 3(f), where a foundry-compatible Si_3N_4 microring with a 450 GHz FSR achieves 3.7 dB of bright two-mode squeezing. After loss correction, the inferred on-chip squeezing level reaches 10.2 dB,[56] marking a significant step toward fault-tolerant CV quantum computing.

4 Integrated Multipartite Entangled Light Sources

CV multipartite entangled states, such as CV cluster states, serve as essential resources for MBQC. MBQC, also referred to as the one-way quantum computing model, differs fundamentally from the general circuit-based model. Instead of performing computation through the sequential application of quantum gates, MBQC relies on the preparation of a highly entangled cluster state followed by feed-forward local measurement results.[13] The larger the entangled resource, the more complex the quantum computing that can be realized. In bulk optics, large-scale CV cluster states have been generated not only through basic path encoding[59,60] but also by multiplexing temporal,[16,17] frequency,[61,62] and spatial modes.[63,64] On the integrated quantum photonic platform, however, generating multipartite entanglement remains challenging. Although second-order single-photon correlations have been observed in soliton microcombs,[65] CV quantum sources typically operate under strong pumping, which excites multiple nonlinear processes within the microresonator. These processes may interact—coupling, cooperating, or competing—complicating the generation and control of on-chip entangled states.

Despite these complexities, recent progress has demonstrated that on-chip multipartite entanglement is indeed achievable. An eight-partite CV entangled state in a microcomb has been demonstrated on a single Si_3N_4 microring using a coherent polychromatic pump-detection (CPPD) technique, as shown in Fig. 4(a).[26] The term "coherent" in the CPPD technique refers to maintaining a stable phase relationship both within and between the multicolor pump light used for generating multipartite entanglement and the multicolor local oscillator (LO) used for balanced homodyne detection (BHD). An electro-optic frequency comb with intrinsic coherence is divided into two groups, as illustrated in Fig. 4(b); the set with the green background is employed for simultaneous polychromatic pumping, whereas the set with the yellow background serves as the multi-frequency LO for polychromatic homodyne detection. Each group of multicolor optical fields remains internally coherent due to propagation in the same spatial mode, whereas inter-group coherence is restored by a chip-external phase-locked loop.

By stabilizing the microring detuning and driving both spontaneous pair squeezing and Bragg scattering processes with the polychromatic pump, an eight-partite entangled state with hidden entanglements is generated. The reconstructed covariance matrix of the frequency qumodes is shown in Fig. 4(c). The reconstruction is carried out via polychromatic homodyne detection, in which—analogous to regular BHD—the signal field and LO field (two spatial modes) are combined on a 50:50 beam splitter and directed to the two photodiodes of a balanced detector. In this scheme, frequency-division multiplexing is applied within each spatial mode, enabling simultaneous measurement across multiple frequency components. To generate a valid CV cluster state,[66] the amplitude and phase of the LO field are adjusted to perform Williamson and Euler decompositions, as shown in Fig. 4(c), thereby decoupling and reconfiguring

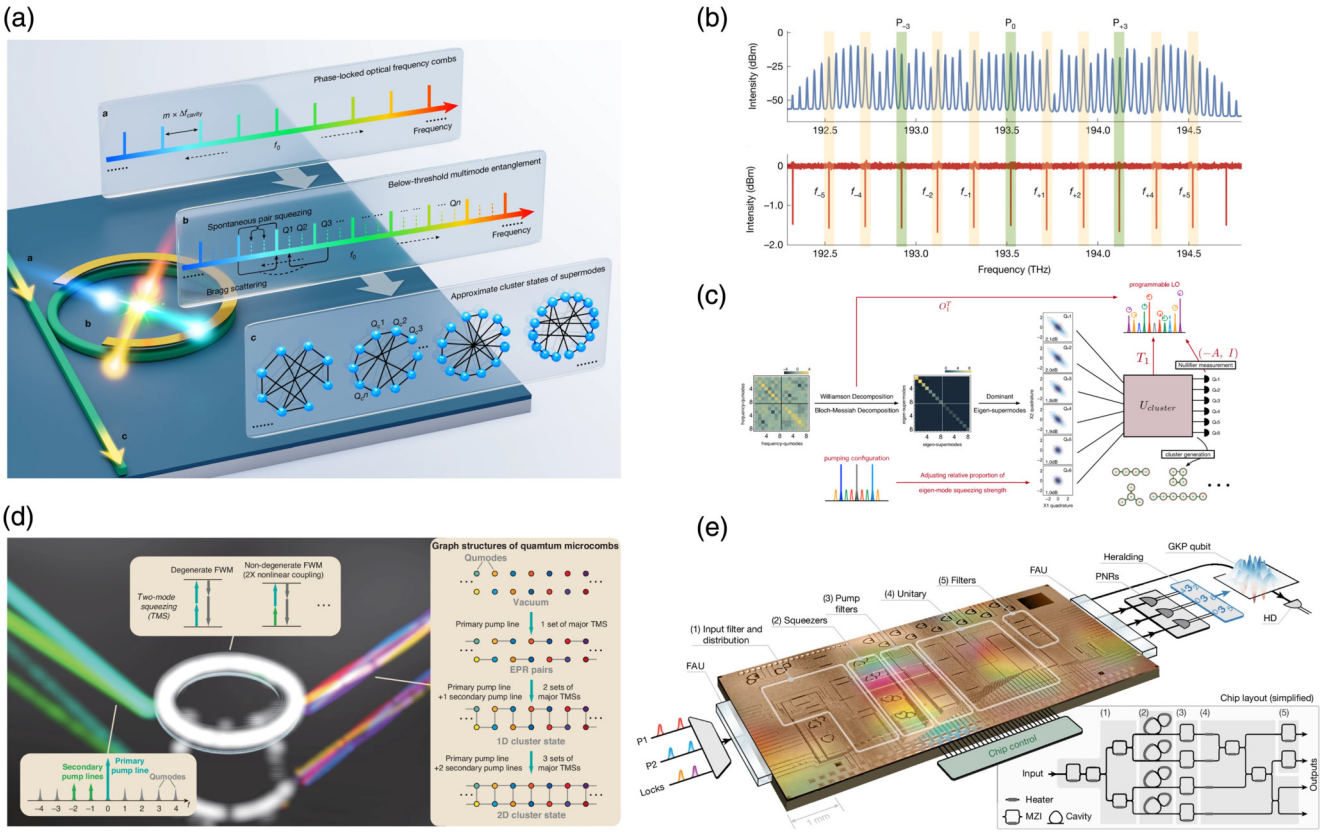

Fig. 4 Typical integrated multipartite entanglement light sources. (a)–(c) CV multipartite entanglement in an integrated microcomb.[26] (a) The processes to generate CV multipartite entanglement with approximate cluster-type structures in the integrated microcomb. (b) Measured spectra of the electro-optic combs and the microring for the CPPD method. (c) The flow for the generation, manipulation, measurement, and characterization of the CV multipartite entanglement state. (d) Schematic of CV cluster quantum microcombs on a SiO_2 resonator.[28] (e) Schematic Si_3N_4 chip layout for on-chip GKP state generation.[33]

inter-mode correlations to obtain eight supermodes of single-mode squeezed states. A subsequent linear transformation facilitated the reconfigurable formation of cluster states with distinct graph structures. Comprehensive characterization of the nullifier correlations and violations of the van Loock–Furusawa criteria confirms the integrated-optic generation of CV cluster states.

This approach of CV cluster-state generation using optical frequency combs is subsequently implemented on a SiO_2 microdisk fabricated on a silicon chip.[28] As shown in Fig. 4(d), by precisely tuning polychromatic pumping, the dimensionality of the resulting cluster states is controllably adjusted, enabling the successful entanglement of 60 quantum modes. The deterministic and on-chip generation of such high-dimensional cluster states represents a promising pathway toward practical, scalable, and universal quantum computing.[67]

Although multiplexed CV cluster states demonstrate scalability, their practical application in universal quantum computing still faces a critical challenge for fault tolerance because CV cluster states suffer from error accumulation during universal operations.[5,14] A promising strategy to overcome this limitation is to hybridize CV cluster states with GKP states, which provide an error-correctable structure within the CV framework.[21,22] The GKP state constitutes a bosonic quantum error-correcting code that protects quantum states against displacement errors in phase space.[68] It has been demonstrated that GKP states can be generated using squeezed cat states in combination with linear optical circuits.[69] Very recently, an optical quantum state synthesizer composed of linear optics and photon-number-resolving detectors, which is commonly referred to as the Gaussian Boson sampling-based approach, has been proposed and realized.[70] Importantly, before photon-number-resolving detection, the output of the Gaussian Boson sampling circuit is a highly structured multipartite entangled Gaussian state, enabling the generation of CV multipartite entangled states on integrated quantum photonic platforms.[33]

As shown in Fig. 4(e), a four-partite CV entangled state is generated by employing a customized multilayer Si_3N_4 300-mm wafer platform optimized for low linear loss and precisely engineered nanophotonic molecule resonators. Spurious nonlinear processes were effectively suppressed, and the output state exhibited a nearly single-temporal-mode form enabled by linear optical transformations. Furthermore, when the chip outputs are coupled via optical fibers to high-efficiency photon-number-resolving detectors, this configuration facilitates the successful generation of a 3×3 lattice GKP state, which exhibits a distinct lattice structure characterized by negative regions in the Wigner function.[33]

5 Discussion and Outlook

Integrated quantum light sources on photonic chips have broad applications in quantum science and technologies, including quantum computation, quantum communication, and quantum sensing. Compared with bulk optical elements, integrated CV photonics have significant advantages in scalability. Specifically, chip-scale integration achieves high component density, enabling the generation and manipulation of large-scale optical modes through frequency or spatial multiplexing. Moreover, the monolithic integration of squeezed light sources with reconfigurable interferometers and detectors further supports the preparation of large-scale CV cluster states and the realization of programmable photonic circuits, which can be applied in quantum networks and communication. In addition, material platforms, such as $LiNbO_3$ and Si_3N_4, provide low-loss and broadband nonlinear interactions with compatibility for various components. Advances in microresonator design, dispersion engineering, and hybrid photonic packaging continue to improve the performance of squeezing level, bandwidth, and noise resilience of integrated CV quantum light sources.

Despite the above promising capabilities, several technical challenges remain toward integrated CV quantum photonic computation architectures. For example, it is essential to develop efficient quantum error correction schemes and improve the squeezing level of CV cluster states for CV MBQC. It has been shown that quantum error correction for CV MBQC can be implemented by encoding bosonic modes into fault-tolerant qubits, such as GKP codes, cat codes, and binomial codes.[71–76] However, MBQC schemes based on GKP encoding typically require a squeezing level of at least 12 dB to satisfy fault tolerance thresholds.[77,78] Achieving on-chip squeezing levels above 10 dB with both high purity and low phase noise is still challenging, particularly under strong pumping conditions. Moreover, integrating low-loss, fast tunable feedforward operations remains technically demanding. Nevertheless, these engineering challenges are expected to be progressively mitigated as fabrication technologies and device integration continue to advance.

To address these limitations, researchers are also exploring new material platforms beyond the mainstream systems, aiming to enhance nonlinear efficiency, integration flexibility, and device functionality. For example, III–V semiconductors, such as AlGaAs, exhibit strong $\chi^{(2)}$ nonlinearities and benefit from mature fabrication technologies.[79] These materials support direct band-gap operation, enabling electrical injection, low-loss optical propagation, large electro-optic responses, and compatibility with superconducting detectors for on-chip photon detection. In addition, aluminum nitride (AlN) features significant $\chi^{(2)}$ nonlinear optical effects, a wide band gap, and a broad transparency window spanning from the ultraviolet to the mid-infrared.[80] It also offers high damage thresholds, along with piezoelectric and pyroelectric properties that make it suitable for integrated optomechanical devices and pyroelectric photodetectors. The integration of these novel materials into established photonic fabrication workflows could unlock new capabilities in CV quantum state engineering.

In summary, we briefly introduce recent experimental breakthroughs in quantum light source engineering, combined with advances in integrated single-mode, two-mode squeezed, and multipartite entangled light sources. It is obvious that a scalable and compelling platform for integrated CV quantum light sources has been established. With ongoing advances in quantum error correction and the squeezing level of CV cluster states, the scalable, universal, and fault-tolerant CV quantum computation is becoming an increasingly realistic and attainable objective.

Disclosures

The authors declare no conflicts of interest.

Acknowledgments

This work is financially supported by the Innovation Program for Quantum Science and Technology (Grant No. 2024ZD0302403), the National Natural Science Foundation of China (Grant No. 12434015), and the Shanxi "1331 Project" Key Subjects Construction.

References

1. U. L. Andersen et al., "Hybrid discrete- and continuous-variable quantum information," *Nat. Phys.* **11**(9), 713–719 (2015).
2. P. van Loock, "Optical hybrid approaches to quantum information," *Laser Photonics Rev.* **5**(2), 167–200 (2011).
3. F. Xu et al., "Entanglement and quantum coherence of hybrid entangled states," *Photonics Res.* **13**, 1983–1990 (2025).
4. F. Xu et al., "Hybrid entanglement carrying orbital angular momentum," *Sci. Bull.* **70**(6), 876–881 (2025).
5. N. C. Menicucci et al., "Universal quantum computation with continuous-variable cluster states," *Phys. Rev. Lett.* **97**(11), 110501 (2006).
6. S. Takeda and A. Furusawa, "Universal quantum computing with measurement-induced continuous-variable gate sequence in a loop-based architecture," *Phys. Rev. Lett.* **119**(12), 120504 (2017).
7. X. Su et al., "Gate sequence for continuous variable one-way quantum computation," *Nat. Commun.* **4**(1), 2828 (2013).
8. M. V. Larsen et al., "Deterministic multi-mode gates on a scalable photonic quantum computing platform," *Nat. Phys.* **17**(9), 1018–1023 (2021).
9. S. D. Bartlett et al., "Efficient classical simulation of continuous variable quantum information processes," *Phys. Rev. Lett.* **88**(9), 097904 (2002).
10. K. Marshall et al., "Quantum simulation of quantum field theory using continuous variables," *Phys. Rev. A* **92**(6), 063825 (2015).
11. T. Honjo et al., "100,000-spin coherent ising machine," *Sci. Adv.* **7**(40), eabh0952 (2021).
12. Y.-H. Deng et al., "Gaussian boson sampling with pseudo-photon-number-resolving detectors and quantum computational advantage," *Phys. Rev. Lett.* **131**(15), 150601 (2023).
13. R. Raussendorf and H. J. Briegel, "A one-way quantum computer," *Phys. Rev. Lett.* **86**(22), 5188–5191 (2001).
14. M. A. Nielsen, "Optical quantum computation using cluster states," *Phys. Rev. Lett.* **93**(4), 040503 (2004).
15. J.-I. Yoshikawa et al., "Invited article: generation of one-million-mode continuous-variable cluster state by unlimited time-domain multiplexing," *APL Photonics* **1**(6), 060801 (2016).
16. M. V. Larsen et al., "Deterministic generation of a two-dimensional cluster state," *Science* **366**(6463), 369–372 (2019).
17. W. Asavanant et al., "Generation of time-domain-multiplexed two-dimensional cluster state," *Science* **366**(6463), 373–376 (2019).
18. C. Roh et al., "Generation of three-dimensional cluster entangled state," *Nat. Photonics* **19**(5), 526–532 (2025).
19. A. A. E. Hajomer et al., "Long-distance continuous-variable quantum key distribution over 100-km fiber with local local oscillator," *Sci. Adv.* **10**(1), eadi9474 (2024).
20. N. P. Mauranyapin, A. Terrasson, and W. P. Bowen, "Quantum biotechnology," *Adv. Quantum Technol.* **5**(9), 2100139 (2022).

21. N. C. Menicucci, "Fault-tolerant measurement-based quantum computing with continuous-variable cluster states," *Phys. Rev. Lett.* **112**(12), 120504 (2014).
22. P. Du et al., "A complete continuous-variable quantum computation architecture based on the 2D spatiotemporal cluster state," *Sci. Rep.* **15**(1), 18199 (2025).
23. E. Pelucchi et al., "The potential and global outlook of integrated photonics for quantum technologies," *Nat. Rev. Phys.* **4**(3), 194–208 (2022).
24. H. Aghaee Rad et al., "Scaling and networking a modular photonic quantum computer," *Nature* **638**(8052), 912–919 (2025).
25. R. Nehra et al., "Few-cycle vacuum squeezing in nanophotonics," *Science* **377**(6612), 1333–1337 (2022).
26. X. Jia et al., "Continuous-variable multipartite entanglement in an integrated microcomb," *Nature* **639**(8054), 329–336 (2025).
27. T. Kashiwazaki et al., "Fabrication of low-loss quasi-single-mode PPLN waveguide and its application to a modularized broadband high-level squeezer," *Appl. Phys. Lett.* **119**(25), 251104 (2021).
28. Z. Wang et al., "Large-scale cluster quantum microcombs," *Light: Sci. Appl.* **14**(1), 164 (2025).
29. M. Stefszky et al., "Waveguide cavity resonator as a source of optical squeezing," *Phys. Rev. Appl.* **7**(4), 044026 (2017).
30. A. Kawasaki et al., "Real-time observation of picosecond-time-scale optical quantum entanglement towards ultrafast quantum information processing," *Nat. Photonics* **19**(3), 271–276 (2025).
31. H. S. Stokowski et al., "Integrated quantum optical phase sensor in thin film lithium niobate," *Nat. Commun.* **14**(1), 3355 (2023).
32. F. Labbé et al., "Thin-film lithium niobate quantum photonics: review and perspectives," *Adv. Photonics* **7**(4), 044002 (2025).
33. M. V. Larsen et al., "Integrated photonic source of Gottesman–Kitaev–Preskill qubits," *Nature* **642**(8068), 587–591 (2025).
34. Y. Zhao et al., "Near-degenerate quadrature-squeezed vacuum generation on a silicon-nitride chip," *Phys. Rev. Lett.* **124**(19), 193601 (2020).
35. C. Bruynsteen et al., "Integrated balanced homodyne photonic–electronic detector for beyond 20 GHz shot-noise-limited measurements," *Optica* **8**(9), 1146–1152 (2021).
36. J. F. Tasker et al., "Silicon photonics interfaced with integrated electronics for 9 GHz measurement of squeezed light," *Nat. Photonics* **15**(1), 11–15 (2021).
37. J. M. Arrazola et al., "Quantum circuits with many photons on a programmable nanophotonic chip," *Nature* **591**(7848), 54–60 (2021).
38. A. I. Lvovsky, *Squeezed Light*, pp. 121–163, Wiley (2015).
39. T. Park et al., "Single-mode squeezed-light generation and tomography with an integrated optical parametric oscillator," *Sci. Adv.* **10**(11), eadl1814 (2024).
40. Y. Zhang et al., "Squeezed light from a nanophotonic molecule," *Nat. Commun.* **12**(1), 2233 (2021).
41. T. Kashiwazaki et al., "Over-8-dB squeezed light generation by a broadband waveguide optical parametric amplifier toward fault-tolerant ultra-fast quantum computers," *Appl. Phys. Lett.* **122**(23), 234003 (2023).
42. A. Kawasaki et al., "Broadband generation and tomography of non-Gaussian states for ultra-fast optical quantum processors," *Nat. Commun.* **15**(1), 9075 (2024).
43. A. Boes et al., "Status and potential of lithium niobate on insulator (LNOI) for photonic integrated circuits," *Laser Photonics Rev.* **12**(4), 1700256 (2018).
44. J. Wang et al., "Integrated photonic quantum technologies," *Nat. Photonics* **14**(5), 273–284 (2020).
45. A. Dutt et al., "On-chip optical squeezing," *Phys. Rev. Appl.* **3**(4), 044005 (2015).
46. Z. Yang et al., "A squeezed quantum microcomb on a chip," *Nat. Commun.* **12**(1), 4781 (2021).
47. J. Yang et al., "Tunable quantum dots in monolithic Fabry–Pérot microcavities for high-performance single-photon sources," *Light: Sci. Appl.* **13**(1), 33 (2024).
48. W. Redjem et al., "All-silicon quantum light source by embedding an atomic emissive center in a nanophotonic cavity," *Nat. Commun.* **14**(1), 3321 (2023).
49. A. Dutt et al., "Tunable squeezing using coupled ring resonators on a silicon nitride chip," *Opt. Lett.* **41**(2), 223–226 (2016).
50. D. Gottesman and J. Preskill, "Secure quantum key distribution using squeezed states," *Phys. Rev. A* **63**(2), 022309 (2001).
51. H. Yonezawa and A. Furusawa, "Continuous-variable quantum information processing with squeezed states of light," *Opt. Spectrosc.* **108**(2), 288–296 (2010).
52. F. Lenzini et al., "Integrated photonic platform for quantum information with continuous variables," *Sci. Adv.* **4**(12), eaat9331 (2018).
53. J. U. Fürst et al., "Quantum light from a whispering-gallery-mode disk resonator," *Phys. Rev. Lett.* **106**(11), 113901 (2011).
54. J. U. Fürst et al., "Low-threshold optical parametric oscillations in a whispering gallery mode resonator," *Phys. Rev. Lett.* **105**(26), 263904 (2010).
55. V. D. Vaidya et al., "Broadband quadrature-squeezed vacuum and nonclassical photon number correlations from a nanophotonic device," *Sci. Adv.* **6**(39), eaba9186 (2020).
56. Y. Shen et al., "Strong nanophotonic quantum squeezing exceeding 3.5 dB in a foundry-compatible Kerr microresonator," *Optica* **12**(3), 302–308 (2025).
57. K. Fukui, "High-threshold fault-tolerant quantum computation with the Gottesman–Kitaev–Preskill qubit under noise in an optical setup," *Phys. Rev. A* **107**(5), 052414 (2023).
58. R. A. Kögler et al., "Quantum state tomography in a third-order integrated optical parametric oscillator," *Opt. Lett.* **49**(11), 3150–3153 (2024).
59. M. Yukawa et al., "Experimental generation of four-mode continuous-variable cluster states," *Phys. Rev. A* **78**(1), 012301 (2008).
60. X. Su et al., "Experimental preparation of eight-partite cluster state with continuous variable entanglement," in *Res. in Opt. Sci., OSA Tech. Digest*, Optica Publishing Group, p. QT1B.3 (2012).
61. M. Chen, N. C. Menicucci, and O. Pfister, "Experimental realization of multipartite entanglement of 60 modes of a quantum optical frequency comb," *Phys. Rev. Lett.* **112**(12), 120505 (2014).
62. Y. Cai et al., "Multimode entanglement in reconfigurable graph states using optical frequency combs," *Nat. Commun.* **8**(1), 15645 (2017).
63. S. Armstrong et al., "Programmable multimode quantum networks," *Nat. Commun.* **3**(1), 1026 (2012).
64. W. Wang, K. Zhang, and J. Jing, "Large-scale quantum network over 66 orbital angular momentum optical modes," *Phys. Rev. Lett.* **125**(14), 140501 (2020).
65. M. A. Guidry et al., "Quantum optics of soliton microcombs," *Nat. Photonics* **16**(1), 52–58 (2022).
66. C. González-Arciniegas et al., "Cluster states from Gaussian states: essential diagnostic tools for continuous-variable one-way quantum computing," *PRX Quantum* **2**(3), 030343 (2021).
67. O. Pfister, "Continuous-variable quantum computing in the quantum optical frequency comb," *J. Phys. B: At. Mol. Opt. Phys.* **53**(1), 012001 (2020).
68. D. Gottesman, A. Kitaev, and J. Preskill, "Encoding a qubit in an oscillator," *Phys. Rev. A* **64**(1), 012310 (2001).
69. S. Konno et al., "Logical states for fault-tolerant quantum computation with propagating light," *Science* **383**(6680), 289–293 (2024).
70. D. Su, C. R. Myers, and K. K. Sabapathy, "Conversion of Gaussian states to non-Gaussian states using photon-number-resolving detectors," *Phys. Rev. A* **100**(5), 052301 (2019).
71. J. Conrad, J. Eisert, and F. Arzani, "Gottesman–Kitaev–Preskill codes: a lattice perspective," *Quantum* **6**, 648 (2022).
72. T. C. Ralph et al., "Quantum computation with optical coherent states," *Phys. Rev. A* **68**(4), 042319 (2003).
73. J. Hastrup and U. L. Andersen, "All-optical cat-code quantum error correction," *Phys. Rev. Res.* **4**(4), 043065 (2022).

74. D. Han et al., "Remote preparation of optical cat states based on Gaussian entanglement," *Laser Photonics Rev.* **17**(9), 2300103 (2023).
75. H. Putterman et al., "Hardware-efficient quantum error correction via concatenated bosonic qubits," *Nature* **638**(8052), 927–934 (2025).
76. M. H. Michael et al., "New class of quantum error-correcting codes for a bosonic mode," *Phys. Rev. X* **6**, 031006 (2016).
77. M. V. Larsen et al., "Fault-tolerant continuous-variable measurement-based quantum computation architecture," *PRX Quantum* **2**, 030325 (2021).
78. I. Tzitrin et al., "Fault-tolerant quantum computation with static linear optics," *PRX Quantum* **2**, 040353 (2021).
79. F. Baboux, G. Moody, and S. Ducci, "Nonlinear integrated quantum photonics with AlGaAs," *Optica* **10**(7), 917–931 (2023).
80. N. Li et al., "Aluminium nitride integrated photonics: a review," *Nanophotonics* **10**(9), 2347–2387 (2021).

Xuezhi Zhu is currently a PhD candidate in optics at Shanxi University. He obtained his BS degree in physics from Shandong Normal University in 2018. His research focuses on CV quantum integrated photonics, CV quantum computing, and quantum sensing.

Siyu Ren received his PhD from Shanxi University in 2023 and has been pursuing postdoctoral studies at Shanxi University since 2023. His research interests are in CV entanglement-assisted quantum communication and CV quantum integrated photonics.

Yunyun Cao is currently a PhD candidate in optics at Shanxi University. She received her BS degree from Shanxi University in 2022. Her research focuses on CV quantum integrated photonics.

Xiaolong Su is currently a professor at Shanxi University. He received his PhD from Shanxi University in 2007. He has published more than 90 journal papers. He is a member of Optica, also serves as editor of *Scientific Reports*, *Science China Information Sciences*, and *Laser Optoelectronics Progress*. His research interests include CV optical quantum information, hybrid optical quantum information, and integrated CV quantum photonics.